DFT study on the mechanism of simultaneous trifluoromethylation and oximation of aryl-substituted ethylene.

Sen Wang[1], Ao He[1], Xuan Meng[1], Xiao wei Lan[1], Xianfu Wei[1], Wenjie Jing[1], Kui Lu[1], and Yujie Dai[1]

[1]Tianjin University of Science and Technology

October 1, 2021

Abstract

The effects of different substituents located at the para position of the aromatic ring and β carbon atom of the styrene on the reaction were investigated. The results showed that the reaction steps with higher energy barriers changed a little with the substituents of the reactants, which indicates that the reaction has a good adaptability to reactants containing different substituents. It was found the proton transfer in the final tautomerism step of nitroso intermediate to oxime is the rate limiting step under anhydrous conditions. Although the solvent effect did not influence the the rate limiting step significantly, the water mediated proton transfer significantly decreased the energy barrier of final tautomerism step. Compared with the direct proton transfer in vacuum, the energy barrier of the final tautomerism step decreased from 57.80kcal/mol in vacuum to 12.98kcal/mol with the water mediated proton transfer in water, which declined by 77.5%. When water participates in rate-limiting steps in organic solvents, the energy barrier also decreases significantly, which indicates that a small amount of water in the organic solvent is conducive to the reaction. This study is of great significance for the application of bifunctionalized reaction in the synthesis of organic fluoride compounds with different substituents.

DFT study on the mechanism of simultaneous trifluoromethylation and oximation ofaryl-substituted ethylene Sen Wang[1], Ao He[1], Xuan Meng[1], Xiaowei Lan[1], Xianfu Wei[1], Wenjie Jing[1], Kui Lu[1], Yujie Dai[1*]

[1]Tianjin Key Laboratory of Industrial Microbiology, Tianjin University of Science and Technology, No.29 of 13th Street, TEDA, Tianjin 300457, PR China;

***Correspondence authors**

Yujie Dai. Tianjin Key Laboratory of Industrial Microbiology, Tianjin University of Science and Technology, No.29 of 13th Street, TEDA, Tianjin 300457, PR China;*yjdai@126.com*;

Present address

Tianjin Key Laboratory of Industrial Microbiology, Tianjin University of Science and Technology, No.29 of 13th Street, TEDA, Tianjin 300457, PR China;

Funding information

This study was financial supported by National Natural Science Foundation of Tianjin, grant No.19JCZDJC34800 and COVID-19 Prevention and Control Project of Tianjin University of Science and Technology (grant No.2020STCV0016).

Astract:

The effects of different substituents located at the para position of the aromatic ring and β carbon atom of the styrene on the reaction were investigated. The results showed that the reaction steps with higher energy barriers changed a little with the substituents of the reactants, which indicates that the reaction has a good adaptability to reactants containing different substituents. It was found the proton transfer in the final tautomerism step of nitroso intermediate to oxime is the rate limiting step under anhydrous conditions. Although the solvent effect did not influence the the rate limiting step significantly, the water mediated proton transfer significantly decreased the energy barrier of final tautomerism step. Compared with the direct proton transfer in vacuum, the energy barrier of the final tautomerism step decreased from 57.80kcal/mol in vacuum to 12.98kcal/mol with the water mediated proton transfer in water, which declined by 77.5%. When water participates in rate-limiting steps in organic solvents, the energy barrier also decreases significantly, which indicates that a small amount of water in the organic solvent is conducive to the reaction. This study is of great significance for the application of bifunctionalized reaction in the synthesis of organic fluoride compounds with different substituents.

Keywords:

Density functional theory; free radical reaction; difunctionalization reaction; trifluoromethylation; oximation.

1.Introduction

Fluorine is an elemental substance with high electronegativity and activity[1]. Introducing the fluorine into the organic molecule can dramatically change its property, such as physical, chemical and biological properties[2]. Especially in the field of pharmaceutical chemistry[3], the introduction of fluorine atoms or fluorine-containing functional groups into the lead compounds has come to the significant research strategies for drug structure optimization[4, 5]. The striking similarity of atomic radii between fluorine and hydrogen allows the fluorine-containing compounds to participate in metabolic response as nature substrate, which is called mimic effect[6]. Therefore, substituting C-F for C-H can change the objective molecule's function and improve its metabolic stability[7].

At present, there are mainly two types of methods introducing the fluorine atom to an organic compound, the direct C-F bond formation[8] and the fluorinated building block method[9]. The first method can be divided into three subtypes according to the regent electrical property: electrophilic-fluorination, nuceleophilic-fluorination and radical-fluorination reactions[10]. Generally, most of these reactions are harsh and difficult to control[11]. The fluorinated building block is an important way for synthesizing fluorinated organic compounds. It uses some fluorinated organic intermediates as fluorinated building blocks to synthesize fluorine-containing target molecules through appropriate reaction pathways[12, 13]. The reaction involving fluorinated building block method generally does not involve the breakdown and formation of C-F bond, and has the characteristics of mild reaction condition, good selectivity and higher yield[14, 15], which favor chemists to it to synthesize fluorine-containing molecules.

Trifluoromethyl has high stability, electronegativity and hydrophobicity. The introduction of trifluoromethyl into a substrate can significantly improve its biological activity[16-18]. Some organic compounds containing trifluoromethyl groups play a very important role in pharmaceuticals, agrochemicals, and organic materials[19]. Some drugs containing trifluoromethyl have come into the market, such as: Efavirenz, Fluoxetine, Celecoxib etc. Trifluoromethylation of substrates has been widely used in the research of new drugs[20]. Therefore, the development of novel methods for the efficient and high selective introduction of the CF_3group into a variety of molecular architectures is highly sought after in the field of synthetic organic chemistry.

In the recent years, various strategies for direct trifluoromethylation of aromatic compounds with copper- and palladium-catalyzed reaction have been well developed[21]. For example, the direct trifluoromethylation of aryl C–H bonds in proximity to directing groups have been individually developed by the groups of Yu[22] and Bräse[23], also introducing trifluoromethyl groups into alkenes has drawn increasing attention[24, 25]. However, this technique need some pre-functionalized alkenes, such as vinyl boronic acids[26], vinyl sulfonates[27], vinyl halides[28], vinyl carboxylic acids[29] or nitro olefins[30] for the preparation of vinyl trifluoromethylates. Although this approach shows good reactivity and regioselectivity, it is cumbersome

and uneconomical due to the pre-activation process. Thus, several new methods for the direct trifluoromethylation of terminal alkenes by employing various trifluoromethyl reagents (e.g., trifluoroalkyl halide, Togni's reagent, and Umemoto's reagent) in the presence of transition metal catalysts have been developed by some scientists[30, 31], including a copper-catalyzed direct trifluoromethylation of vinyl C–H bonds of styrene derivatives with CF_3SO_2Na (Langlois reagent).

The oxime structural motif is existed widespread in natural products[32, 33] or some biologically active compounds[34, 35]. It is an important synthon as versatile precursors in the syntheses of amines[36, 37], amides[38], nitriles[36, 39], and heterocyclic compounds[40]. Though there are a variety of synthetic methods have been developed for the preparation of oximes, they usually need the existence of carbonyl or nitro in the substrate[41, 42].

Simultaneously introducing two functional groups into aryl olefin molecules can significantly simplify the reaction steps and shorten the preparation time, thus improve the atomic economy of the reaction atoms and reduce waste emissions. It has been reported that α-sulfonyl ketoximes could be prepared with the reaction of 1,2-difunctionalisation of styrenes with sodium arylsulfinates and tert-butyl nitrite (TBN)[43, 44]. Our group previously investigated the bifunctionalization reaction of aryl-substituted ethylene with Langlois reagent (CF_3SO_2Na) as trifluoromethylation reagent and tert-butyl nitrite (TBN) as oxidant and oxime source, which introduced a trifluoromethyl and an oxime simultaneously at the double bond position. Based on NMR and isotope tracking experiments, the following putative reaction mechanism was proposed[45] (Scheme 1):

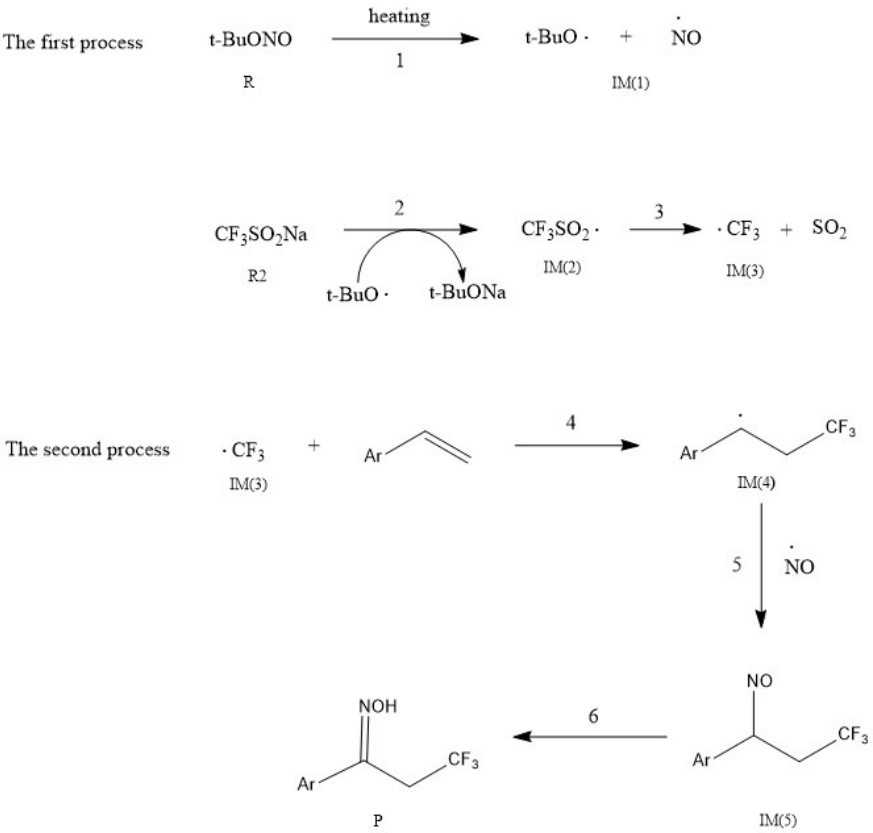

Scheme 1. The putative reaction mechanism of simultaneous trifluoromethylation and oximation of substituted styrene.

It includes 6 steps which can be divided into 2 processes. However, the transition states, the reaction rate constants, the rate limiting step, and the energy change in the reaction process have not been clearly understood. Therefore, in order to further comprehend the mechanism of the reaction in detail so as to better expend its application. In this study the quantum chemistry calculation was employed to examine the transition state and energy change of each step of the reaction. The reaction rate limiting step was examined and the effects of the solvents and substituent groups were also examined.

Computational methods

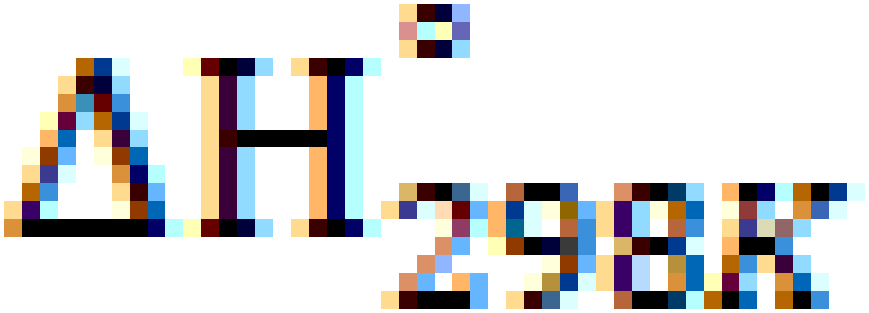

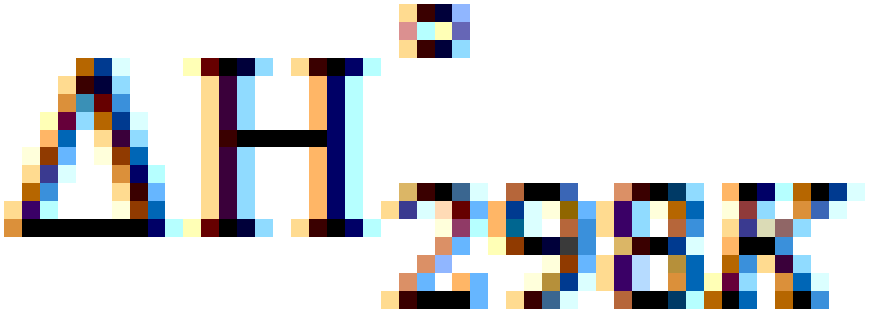

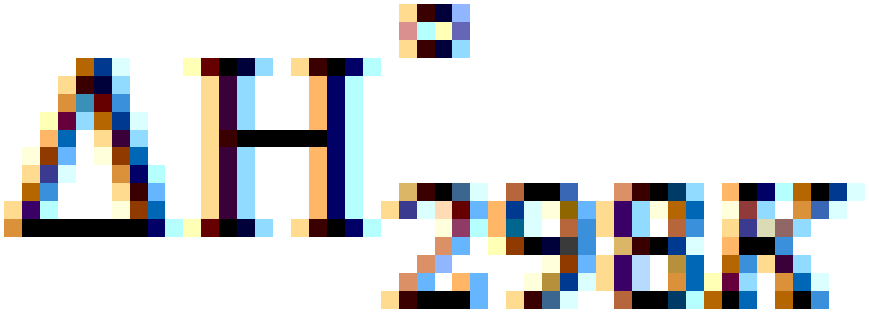

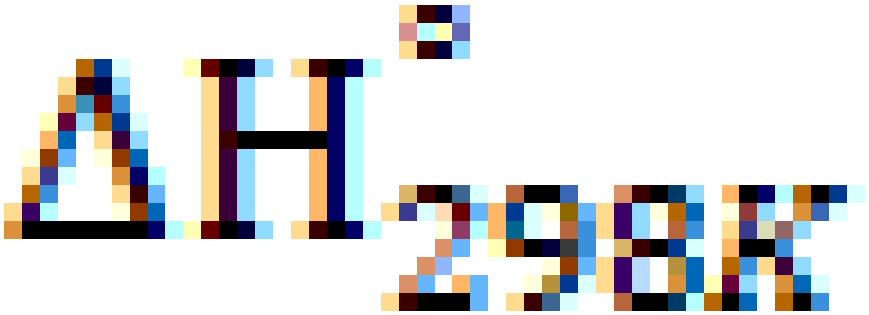

All of the quantum chemistry computation and structure optimization of the reactant, product and the transition state were based on the density functional theory(DFT)[46]. All the computations were performed with the Gaussian09 package[47]. All molecular geometries including reactants, intermediates and products in the reactions in vacuum and in the solvents of DMSO, ethanol and water respectively were optimized at the B3LYP/6-31+G(d, p) level. The solvent effects were simulated using the CPCM model[48]. Unrestricted spin calculations were used for all the open–shell systems. The TS and QST2 methods were used to find the transition states when the structures of the reactant and the product in the reaction were fully optimized. Frequency analyses were conducted to determine whether a given structure is a minimum or a transition state. Calculations of intrinsic reaction coordinates (IRC) were employed to confirm the located transition states which connect with the expected minima. All initial states, stable intermediates and final products were confirmed to have only real harmonic frequencies and each transition state was confirmed to have one single imaginary vibrational[49]. The energy barrier of the reaction was obtained from the energy difference between the transition states and the corresponding reactants with the zero-point correction. The reaction enthalpy change () and Gibbs free energy change() of reactions can be obtained from the difference in enthalpy and Gibbs free energy between the products and the corresponding reactants. Transition state theory is often used to calculate the chemical reaction rate constants(k)[50] and in this paper, we calculated the reaction rate constant using the following formula[51, 52]:

$$k = \frac{\kappa \cdot \sigma \cdot k_b \cdot T}{h} \cdot \frac{Q_{\mathrm{TS}}}{Q_A} \cdot e^{\left(\frac{-E}{R \cdot T \cdot 1000}\right)} (1)$$

$$\kappa = 1 + \left(\frac{h}{k_b \cdot T \cdot \zeta_{\mathrm{fre}} \cdot 3 \times 10^{10}}\right)^{\frac{2}{24}} (2)$$

$$k = \frac{\kappa \cdot \sigma \cdot k_b \cdot T}{h} \cdot \frac{k_b \cdot T}{P} \cdot 10 \cdot \frac{Q_{\mathrm{TS}}}{Q_A \cdot Q_B} \cdot e^{\left(\frac{-E}{R \cdot T \cdot 1000}\right)} (3)$$

In the above formula,k_b, h, R, P and T are physical constants. k_b is the Boltzmann constant (equels to 1.38×10^{-23}J·K^{-1}). h is the Planck constant (6.63×10^{-34} J·s). R is the molar gas constant (8.314 J/(mol·K)). P is the pressure(bar). T is the reaction temperature (298K). σ is the degree of degeneracy of the reaction path (the value is 1 in this study). E is the static potential threshold on the minimum energy response path (MEEP).Q_A and Q_B are the partition functions of the reactants andQ_{TS} is the partition function for the transition state[53]. ζ_{fre} is the imaginary frequencies of the transition state. Equation (1) is used to calculate the monomolecular reaction rate. $\varkappa$ is the tunnel effect correction factor, which can be calculated by the equation (2). Equation (3) is used to calculate the bimolecular reaction rate. In equation (3) we multiply N_A*0.001 when convert unit ($s^{-1}(molec/cm^3)^{-1}$) to unit ($s^{-1}M^{-1}$). $N_A$is the Avogado constant. All the 3D molecular structures were made by GaussView 5.0[54].

Results and discussion

The formation of trifluoromethyl radicals in vacuum.

The proposed reaction process for the simultaneous trifluoromethylation and oximation of aryl-substituted

ethylene has been given in Scheme 1. The whole reaction process is a free radical reaction. The reaction can be divided into two process including 6 steps: (1) TBN(Tert-butyl nitrite) is broken up into tert-butanol radical and nitric oxide radical by heating. The former acts as an oxidant and the later acts as an oxime in the subsequent steps. The radical transfer from tert-butanol radical to Langlois reagent(CF_3SO_2Na) to form trifluoromethylsulfinic radical, followed by the homolysis to give the trifluoromethyl radical. (2) The process includes steps 4 5 and 6 for the aryl substituted ethylene reacts with the intermediates (trifluoromethyl radical and nitric oxide radical, which were generated from the first two processes) to give the α-trifluoromethylethylketoxime. The formation of trifluoromethyl radicals include 3 steps and the optimized structure parameters of reactants (R), transition states(TS) and intermediates(IM) in vacuum and in the dimethyl sulfoxide (DMSO), ethanol and water are shown in Figures 1 and 2. The potential energy surface of the formation of trifluoromethyl radicals process in vacuum was given in the Figure 4.

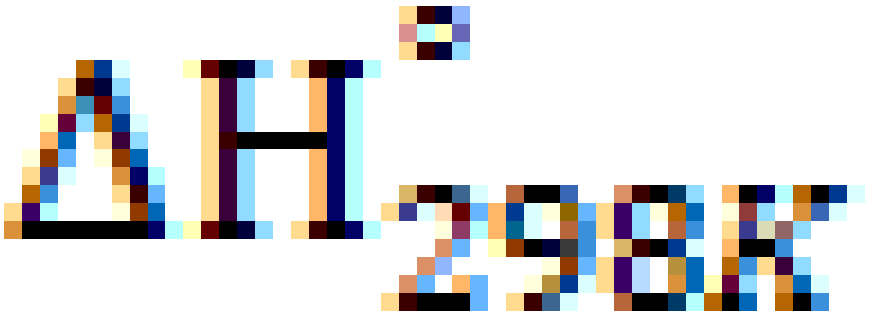

Figure. 1. Some optimized structural parameters in reactant (R) and transition state (TS) of TBN homolysis in vacuum(Oxygen:red; Nitrogen:blue; Carbon:gray; Hygrogen: white).

The bond length of N(6) to the O(5) was 1.398Å and the distance of C(1)-O(5) was 1.481Å in tert-butyl nitrite (R). The distance of nitrogen-oxygen double bond was 1.188Å. The angle for O(7)-N(6)-O(5) was 110.909°. With the reaction went on, N(6) atom of TBN took away from the O(5) atom, and the transition state(TS) was formed with 1.654Å of the bond length for N(6)-O(5) and the length of the N(6)=O(7) became 1.196Å. The angle for O(7)-N(6)-O(5) became 116.579° in TS(1) and the angle was increased by 5.67° compared with the reactant. As the reaction further went on, the distance of N(6) and O(7) stretched further and with the bond broken, the NO and tert-butanol radical was formed. The subsequent step is the formation of trifluoromethyl radical, which is an important process for the simultaneous trifluoromethylation and oximation of aryl-substituted ethylene. The step 2 is triggered by t-BuO· attacking the sodium atom to form trifluoromethyl sulfonate radical and sodium tert-butoxide. Simultaneously, the C(1)-S(5) bond in trifluoromethyl sulfonate radical is lengthened from 1.905Å to 1.953Å and the O(6)-S(5)-O(7) bond angle increases from 118.431° to 122.489° in IM(2) (as shown in Figure 2). Subsequently in step 3, the length of the C(1)-S(5) bond is further extended to 2.669Å to form the transition state (TS(2)) and finally C(1)-S(5) bond breaks to form trifluoromethyl radical and sulfur dioxide. This reaction is a radical transfer reaction.

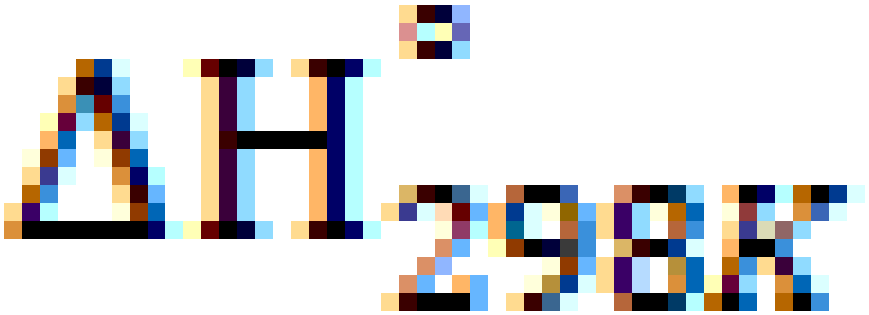

Figure 2. The optimized initial and transition state structures (IM2 and TS(2)) in the homolysis of trifluoromethyl sulfonate radical to form trifluoromethyl radical in vacuum(Oxygen:red; Sulfur:yellow; Carbon:gray; Fluorine:cyan).

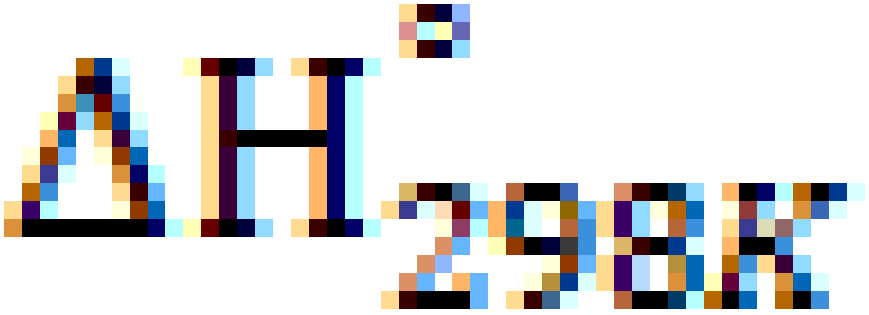

Figure 3. The potential energy surface scanning of the distance between O(8) of tert-butyl radical and Na(9) of sodium trifluoromethyl sulfonate in step 2 in vacuum. (a: energy change in the potential energy surface scanning; b: molecular structure of a frame during scanning: $D_{O(8)\text{-}Na(9)}$: the distance between O(8) of tert-butyl radical and Na(9) of sodium trifluoromethyl sulfonate. (Oxygen:red; Sulfur:yellow; Carbon:gray; Fluorine:cyan; Sodium:purple; Hygrogen: white).

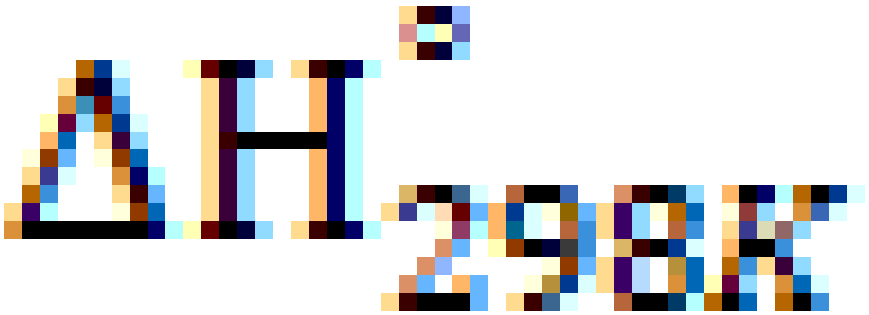

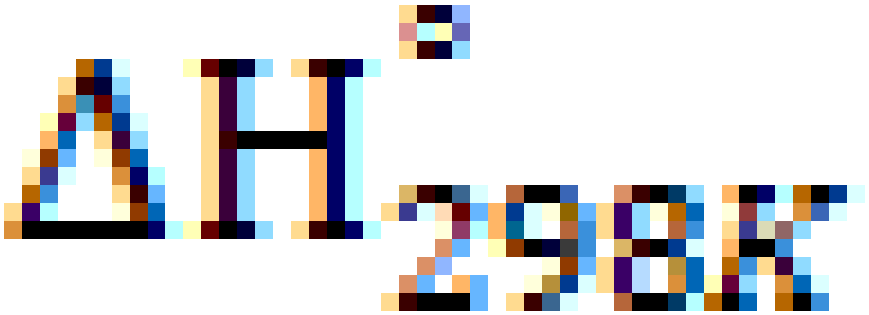

It can be seen from Table 1 that the energy barrier of the homolysis of TBN was 47.42kal/mol which was obtained from the relative energy difference between the transition state of TS(1) and the reactant TBN(R). This reaction is endothermic and the amount of heat absorbed is 35.32kcal/mol depending on the relative energy difference between the intermediate of IM(1) and TBN(R). The reaction rate constant of the homolysis of TBN is $7.699\times10^{-24}s^{-1}$(given in Table 1). As shown in Table 1, this sodium transfer of step 2 is endothermic and the reaction enthalpy change () is 29.78kcal/mol. The potential energy surface scanning (shown in Figure 3) shows that there is no energy maximum point during the sodium move from $CF_3SO_2\cdot$ to t-BuO·. It is a barrierless step without transitions states. It can be considered that the reaction of this step is controlled by diffusion with a very fast reaction rate. Subsequently, the generated $CF_3SO_2\cdot$ was homolyzed in step 3 to give the $\cdot CF_3$ and SO_2. This step is a Gibbs free energy decrease process. As shown in the Table 1, the energy barrier with the breakage of C-S bond in $CF_3SO_2\cdot$ homolysis is 5.68kcal/mol and the reaction rate constants of this step is $2.973\times10^{7}s^{-1}$. The low energy barriers and high reaction rate constants of this step indicate that this step can be conducted under normal temperature very easily. As a whole, the generation of $\cdot CF_3$ initialed by t-BuO· can be carried out at room temperature readily. The products of this process include trifluoromethyl radical and nitric oxide (NO) and they continue to act as an intermediate reactant to react with aryl substituted ethylene. It can be seen from Table 1 that the breakage of C-S bond is an endothermic process and the reaction enthalpy change is 4.24kcal/mol. In sum, The reactions including step 1, 2 and 3 in the first process are all endothermic steps.

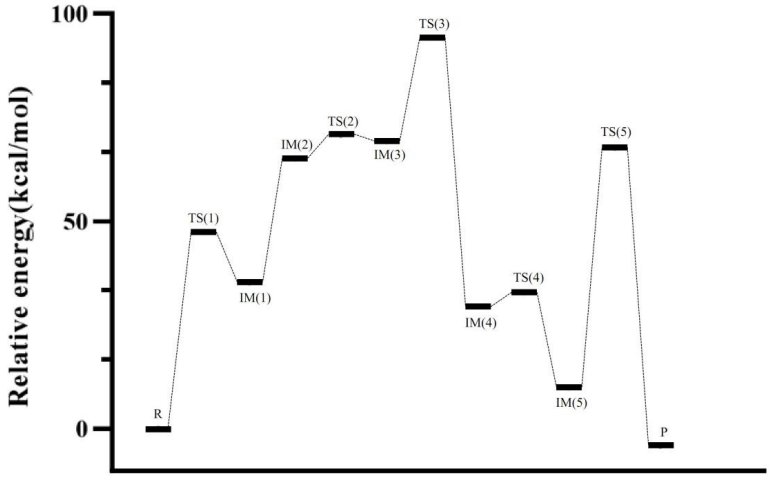

Figure 4. the potential energy surface of the difunctionalization reaction of aryl-substituted ethylene in vacuum.

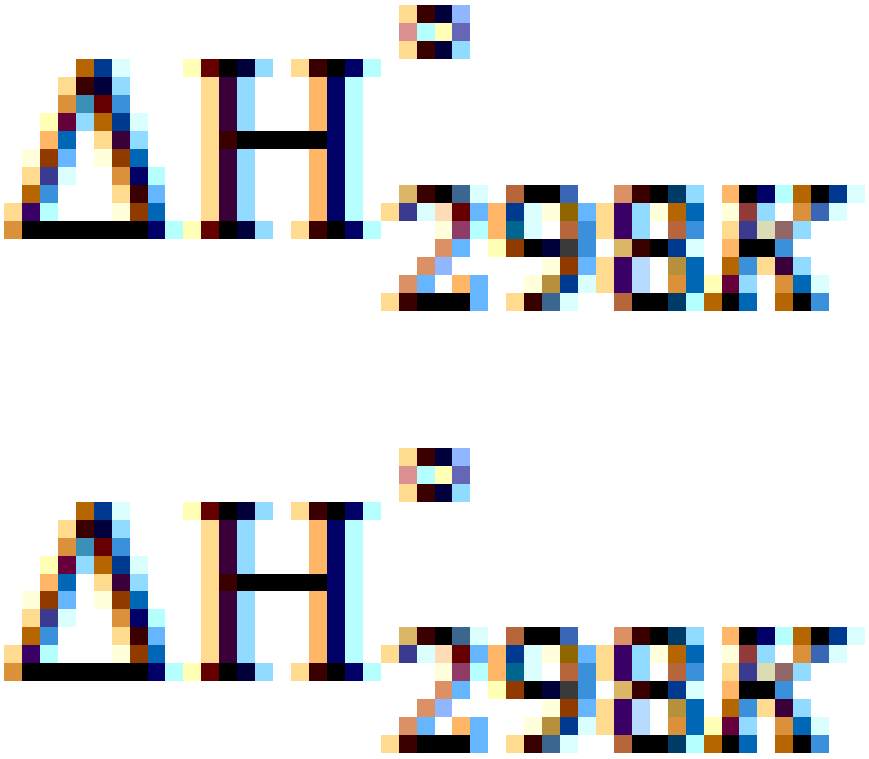

Table 1. The energy barriers([?]E*)* , reaction enthalpy changes(), Gibbs free energy changes($G"C_{298K}$), tunneling correction factors ($\varkappa$) and reaction rate constants(k) of the six reaction steps corresponding to those in Scheme 1.

Step	*[?]E*(kcal/mol)	(kcal/mol)	(kcal/mol)	$\varkappa$	k
1 V	47.42	35.32	24.41	1.1771	$7.699\times10^{-24}s^{-1}$
1 D	47.88	35.10	24.21	1.184	$3.558\times10^{-24}s^{-1}$
1 E	47.86	35.11	24.13	1.184	$3.680\times10^{-24}s^{-1}$
1 W	47.88	35.10	24.21	1.184	$3.558\times10^{-24}s^{-1}$
2 V	-	29.78	28.69	-	-
2 D	-	27.35	26.96	-	-
2 E	-	27.27	25.77	-	-
2 W	-	27.36	27.21	-	-
3 V	5.68	4.24	-7.07	1.006	$2.973\times10^{7}s^{-1}$
3 D	4.97	3.20	-7.95	1.004	$9.859\times10^{7}s^{-1}$
3 E	4.99	3.22	-7.93	1.004	$9.531\times10^{7}s^{-1}$
3 W	4.96	3.19	-9.84	1.004	$1.002\times10^{8}s^{-1}$
4 V	24.84	-39.96	-27.97	1.006	$1.952\times10^{-12}s^{-1}M^{-1}$
4 D	25.59	-40.53	-28.91	1.003	$5.477\times10^{-13}s^{-1}M^{-1}$
4 E	25.58	-40.51	-28.88	1.003	$5.569\times10^{-13}s^{-1}M^{-1}$
4 W	33.64	-40.53	-28.93	1.003	$6.704\times10^{-19}s^{-1}M^{-1}$

Step	[?]E(kcal/mol)	(kcal/mol)	(kcal/mol)	$\varkappa$	k
5 ^{V}	3.49	-19.37	-8.35	1.080	$1.003\times10^{4}s^{-1}M^{-1}$
5 ^{D}	1.56	-20.69	-9.23	1.036	$2.516\times10^{5}s^{-1}M^{-1}$
5 ^{E}	1.61	-20.66	-9.22	1.037	$2.314\times10^{5}s^{-1}M^{-1}$
5 ^{W}	1.54	-20.27	-9.24	1.035	$2.600\times10^{5}s^{-1}M^{-1}$
6 ^{V}	57.80	-13.98	-11.72	6.170	$9.607\times10^{-31}s^{-1}$
6 ^{D}	58.36	-14.95	-12.73	6.244	$3.771\times10^{-31}s^{-1}$
6 ^{E}	58.36	-14.93	-12.71	6.244	$3.771\times10^{-31}s^{-1}$
6 ^{W}	58.36	-14.96	-12.74	6.244	$3.771\times10^{-31}s^{-1}$

* ^{D}:DMSO; ^{E}: ethanol;^{V}: in vacuum; ^{W}: water ; -: not obtained.

3.2 Τηε προcεσς οφ τριφλυορομετηψλ ραδιcαλ αττασκινγ στψρενε το προδυcε α-τριφλυορομετηψλ ετηψλ κετοξιμε ιν ασυυμ.

In this paper, styrene is used as the initial representative of aryl substituted ethylene. It is an important monomer of synthetic resin and an important industrial raw material to prepare ion exchange resin and synthetic rubber in industry. In addition, styrene can also be used in pharmaceutical, dyes, pesticides and mineral processing industries[55]. Trifluoromethyl is often used as a bioisostere in place of chlorine or methyl in the preparation of some derivatives. It can be used to regulate the configuration and electronic properties of lead compounds or to protect active methyl groups from metabolic oxidation[56]. Trifluoromethyl radical is commonly used to synthesize trifluoromethyl functional groups. In this research, the addition of trifluoromethyl group to the C=C double bond of styrene and the subsequent reactions were explored.

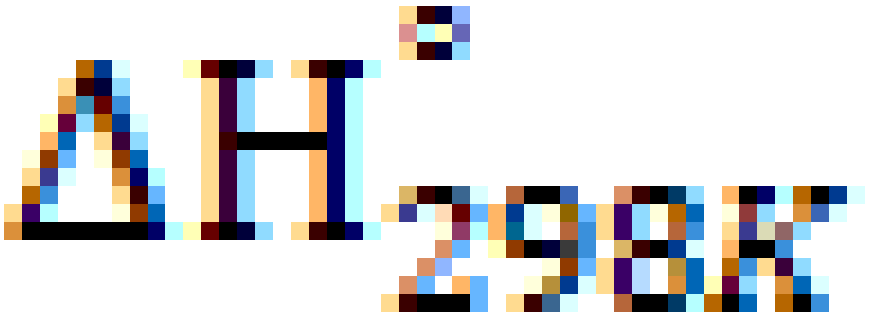

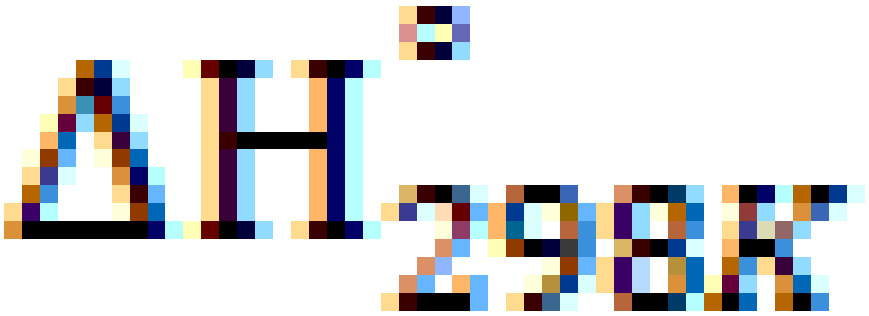

Process 2 in scheme 1 mainly has three steps and includes steps 4 5 and 6. The step 4 is that trifluoromethyl radical (IM(3)) attacks styrene to generate (3,3,3-trifluoropropyl)benzene radical intermediate(IM(4)). As shown in Figure 5, before the trifluoromethyl radical attacked styrene, the length of the C(2)=C(8) bond was 1.341Å and in the TS(3) it became 1.348Å. In the intermediate of IM(4), the newly formed bond(C(8)-C(9)) was 1.514Å, the old bond(C(2)=C(8)) became C(2)-C(8) that has a bond length of 1.499Å and the single bond between C(2) and C(1) was shortened to 1.415Å. Steps of 5 and 6 are that (3,3,3-trifluoropropyl)benzene radical intermediate(IM(4)) reacts with the nitric oxide free radical produced by the hemolysis of TBN to generate 3,3,3-trifluoro-1-phenylpropan-1-nitric oxide(IM(5)), which converts the α-trifluoromethylethyl ketoxime(P) through the tautomerism reaction. In the transition state TS(4), the bond length of C(1)-C(2) changes from 1.415Å in IM(4) to 1.446Å and the bond length of C(2)-N(21) is 2.033Å. And the new bond C(2)-N(21) in IM(5) has a bond length of 1.526Å. Subsequently, the isomerization reaction took place, which was the transfer of H(13) from C(2) to O(22). With H(13) atom of C(2) further approaching the O(22) atom of nitric oxide, an product structure of α-trifluoromethylethyl ketoxime (P) was formed. From the transition state structure of reaction step 6 shown in Figure 5, it can be seen that a four atom cyclic transition state (TS(5)) with C(2), H(13), O(22) and N(21) formed for H(13) transfer between the C(2) and O(22), and with the reaction went on, the distance between N(21) and O(22) stretched from 1.283Å in IM(5) to 1.396Å in α-trifluoromethylethyl ketoxime(P) and the single bond between N(21) and C(2) reduced from 1.391Å to 1.288Å. The new bond O(22)-H(13) in α-trifluoromethylethyl ketoxime(P) has a length of 0.967Å. That's the end of the whole reaction. It can be seen that from the Table 1, the step 4 of trifluoromethyl radical attacking styrene to generate (3,3,3-trifluoropropyl)benzene radical(IM(4)) is an exothermic reaction and the reaction heat() is -39.96kcal/mol. The energy barrier of step 4 is 24.84kcal/mol and the reaction rate constant is $1.952\times10^{-12}s^{-1}M^{-1}$. Subsequently, the step 5 is that IM(4) took an addition reaction with nitric oxide free radical. The energy barrier of the fifth step is the smallest in the second process, which is 3.49kcal/mol and the reaction rate constant is $1.003\times10^{4}s^{-1}M^{-1}$. And the fifth step is also an exothermic reaction, and the enthalpy change of the reaction is -19.37kcal/mol. As shown in Table 1, the energy barrier for H(13) transferring from C(2) to O(22) was 57.80kcal/mol. Compared with other steps, step 6 has the highest energy barrier and is the rate-limiting step for the whole reaction process. It can be seen from Table 1 that the rate constants for this rate-limiting step is $9.607\times10^{-31}s^{-1}$. Step 6 is also an exothermic process and the enthalpy change is -13.98kcal/mol.

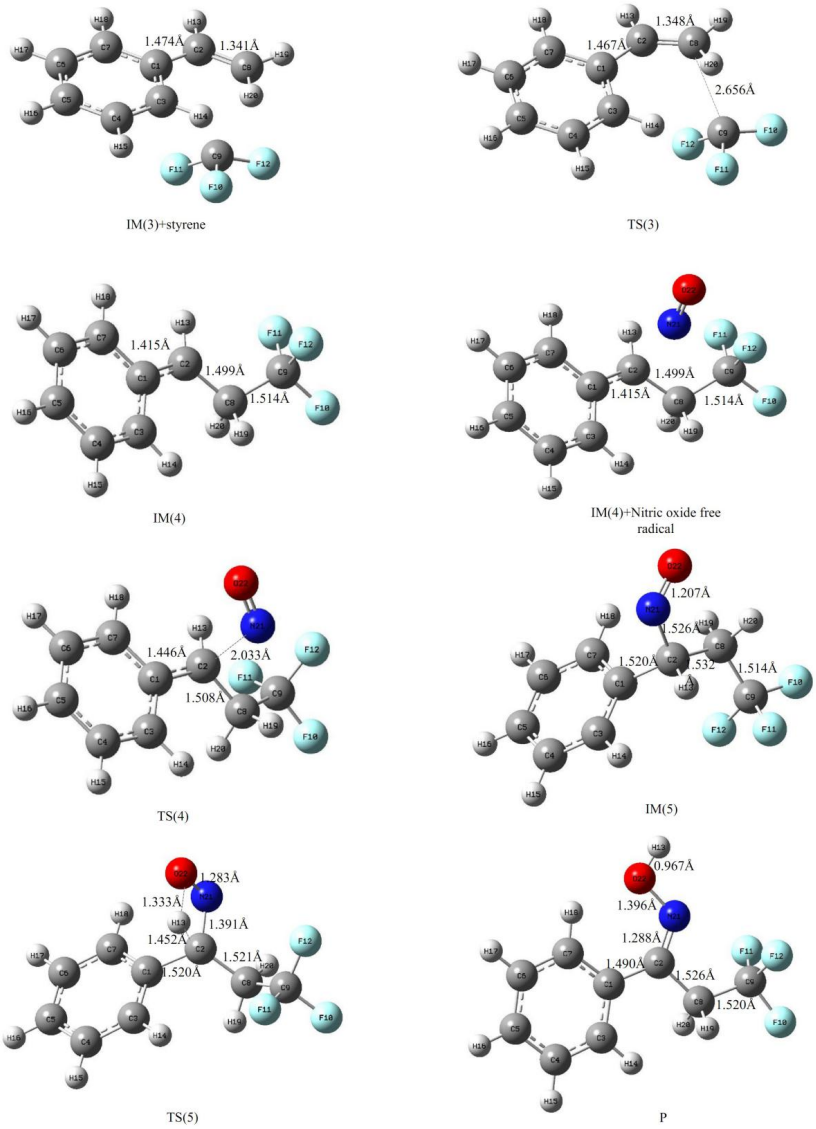

Figure 5. The optimized structure and some main parameters of the intermediates(IM), transition states(TS) and products(P) in steps of 4 5 and 6 of the difunctionalization reaction of styrene in vacuum(Oxygen:red; Nitrogen:blue; Carbon:gray; Fluorine:cyan; Hygrogen: white).

3.3 Effect of the para substituents of aryl ring and the β-substituents of styrene on the difunctionalization reaction in acuum.

The substituents on the aromatic ring of styrene can affect the electron density distribution of benzene ring and conjugated vinyl bond, and further may affect the difunctionalization reaction. Grainger R *et al.* [57] reported that the ortho substituents close to the reaction sites may have some influence on the formation of

transition states. The electron-donating and the electron-withdrawing substituents have the different effect on the electron distribution of the reactants and transition states, and further influence the energy barrier of the reaction[58]. In order to examine the effect of para substituents of the aryl ring on the difunctionalization reaction, the difunctionalization reactions of the para substituted styrene with the electron-donating groups of methoxyl, methyl and the withdrawing group of fluorine were examined in this study. To further explore the effect of substituents on the difunctionalization reaction, the effect of β-carbon substituents on the reaction were also investigated. We chose methoxy and fluorine as representatives of the electron-donating and withdrawing groups respectively at theβ-C substituents of styrene to explore the effects of substituents on the difunctionalization reaction. Since the first process only produces trifluoromethyl radical and does not involve the subsequent reaction of styrene, the substituents only affect the second process. So in this section, the reaction steps of 4 5 and 6 of the difunctionalization reaction with the substituted styrene were examined. Table 2 and Table 3 list the energy barriers needed to be overcome and the reaction rate constants for the reaction steps of 4 5 and 6 of difunctionalization reactions of substituted styrenes. Figure 6 shows the optimized structure and some main parameters of the intermediates, transition states and products in steps of 4 5 and 6 of the difunctionalization reaction of para substituted styrene at B3LYP/6-31+G(d, p) level in vacuum. The corresponding structural parameters of the intermediates, transition states and products in steps of 4 5 and 6 of the β-C substituted styrene in the difunctionalization reaction in vacuum are listed in Figure 7.

Table 2. The energy barriers (*[?]E* $_4$,*[?]E* $_5$ and *[?]E* $_6$) and reaction rate constants (k_4, k_5 and k_6) of steps of 4 5 and 6 for the para-substitued styrenes in vaccum (^{V}) and different solvents of DMSO (^{D}), ethanol(^{E}) and water(^{W}).

Substituents	[?]E_4 (kcal/mol)	(k_4) ($s^{-1}M^{-1}$)	[?]E_5 (kcal/mol)	(k_5) ($s^{-1}M^{-1}$)	[?]E_6 (kcal/mol)	(k_6) (s^{-1})
Methoxyl ^{V}	0.03	3.242×10^{6}	1.51	2.791×10^{5}	58.10	5.780×10^{-31}
Methoxyl ^{D}	0.26	2.188×10^{6}	0.92	7.333×10^{5}	58.56	2.679×10^{-31}
Methoxyl ^{E}	0.21	2.381×10^{6}	0.96	6.853×10^{5}	58.43	3.337×10^{-31}
Methoxyl ^{W}	0.21	2.382×10^{6}	0.93	7.203×10^{5}	58.43	3.338×10^{-31}
Methyl ^{V}	25.01	1.462×10^{-12}	3.11	1.904×10^{4}	57.92	7.849×10^{-31}
Methyl ^{D}	25.76	4.107×10^{-13}	0.95	7.031×10^{5}	58.39	3.574×10^{-31}
Methyl ^{E}	25.76	4.107×10^{-13}	1.02	6.252×10^{5}	58.39	$3.575\times10^{-31}s^{-1}$
Methyl ^{W}	25.77	4.035×10^{-13}	0.93	7.273×10^{5}	58.39	$3.574\times10^{-31}s^{-1}$
F ^{V}	30.34	1.783×10^{-16}	3.48	1.019×10^{4}	58.08	6.002×10^{-31}
F ^{D}	31.38	3.066×10^{-17}	1.52	2.692×10^{5}	58.63	2.397×10^{-31}
F ^{E}	31.36	3.171×10^{-17}	1.58	2.435×10^{5}	58.63	2.396×10^{-31}
F ^{W}	31.39	3.014×10^{-17}	1.49	2.829×10^{5}	58.63	2.397×10^{-31}

Table 3. The energy barriers (*[?]E* $_4$,*[?]E* $_5$ and *[?]E* $_6$) and reaction rate constants (k_4, k_5 and k_6) of steps of 4 5 and 6 for the β-C substituents of styrenes in vaccum (^{V}) and different solvents of DMSO (^{D}), ethanol(^{E}) and water(^{W}).

Substituents	[?]E_4 (kcal/mol)	(k_4) ($s^{-1}M^{-1}$)	[?]E_5 (kcal/mol)	(k_5) ($s^{-1}M^{-1}$)	[?]E_6 (kcal/mol)	(k_6) (s^{-1})
Methoxyl ^{V}	27.95	1.048×10^{-14}	6.64	4.834	58.25	4.438×10^{-31}
Methoxyl ^{D}	28.84	2.323×10^{-15}	4.83	1×10^{3}	58.37	3.678×10^{-31}
Methoxyl ^{E}	28.60	3.472×10^{-15}	4.88	9.189×10^{2}	58.37	3.677×10^{-31}
Methoxyl ^{W}	28.63	3.300×10^{-15}	4.80	1.051×10^{3}	58.38	3.617×10^{-31}
F ^{V}	31.27	3.829×10^{-17}	7.34	1.510	57.00	3.612×10^{-30}
F ^{D}	32.01	1.092×10^{-17}	6.24	9.445	57.53	1.502×10^{-30}

Substituents	[?]E_4 (kcal/mol)	(k_4) ($s^{-1}M^{-1}$)	[?]E_5 (kcal/mol)	(k_5) ($s^{-1}M^{-1}$)	[?]E_6 (kcal/mol)	(k_6) (s^{-1})
F ^{E}	31.68	1.914×10^{-17}	6.27	8.986	57.52	1.527×10^{-30}
F ^{W}	31.72	1.784×10^{-17}	6.22	9.770	57.53	1.502×10^{-30}

Table 2 shows the energy barrier change of the second process with the different para substituents on the aryl ring of styrene. When the substituent was electron-donating substituent -CH_3O in the para-positon, the reaction energy barrier of step 4 directly decreased from 24.84kcal/mol (H) to 0.03kcal/mol (-CH_3O), which decreased by 24.81kcal/mol and the reaction rate constant went from $1.952\times10^{-12}s^{-1}M^{-1}$to $3.242\times10^{6}s^{-1}M^{-1}$. But the electron-withdrawing substituent F increased the energy barrier of step 4 by 5.50kcal/mol in vacuum. Among all substituents, methoxy group has the greatest influence on the step 5, decreasing the reaction energy barrier by 1.98kcal/mol and the reaction rate constant from $1.003\times10^{4}s^{-1}M^{-1}$increases to $2.791\times10^{5}s^{-1}M^{-1}$. It can be seen that the substituents have little effect on step 5, though both the electron-donating substituent and electron-withdrawing group decreased the reaction energy barriers. For step 6, it is the rate limiting step. Both the electron-donating substituents and the electron-withdrawing substituents increased little of the energy barrier in vacuum and the maximum increase was only 0.30kcal/mol with the existence of methoxy.

Compared the data in Table 3 with that in Table 1, the reaction barriers of steps 4 and 5 increase both with the presence of methoxy and fluorine asβ-C substituents. When the methoxy group is located atβcarbon, the reaction energy barrier of step 4, 5 and 6 was increased by 3.11kcal/mol 2.95kcal/mol and 0.45kcal/mol respectively in vacuum. Fluorine has a greater effect on the energy barrier, which increasee the reaction energy barriers of steps 4 and 5 by 6.43kcal/mol and 3.85kcal/mol respectively. For the rate-limiting step, substituent F located at β carbon reduces the reaction barrier only by 0.8kcal/mol. We know that the rate-limiting step of the reaction plays a decisive role in the reaction. As a whole, for para and β-carbon substituents, neither the electron-withdrawing substituents nor the electron-donating substituents have much effect on step 6, indicating that the difunctionalization reaction has good applicability for substituted styrene derivatives with different substituents at para and β-carbon positions.

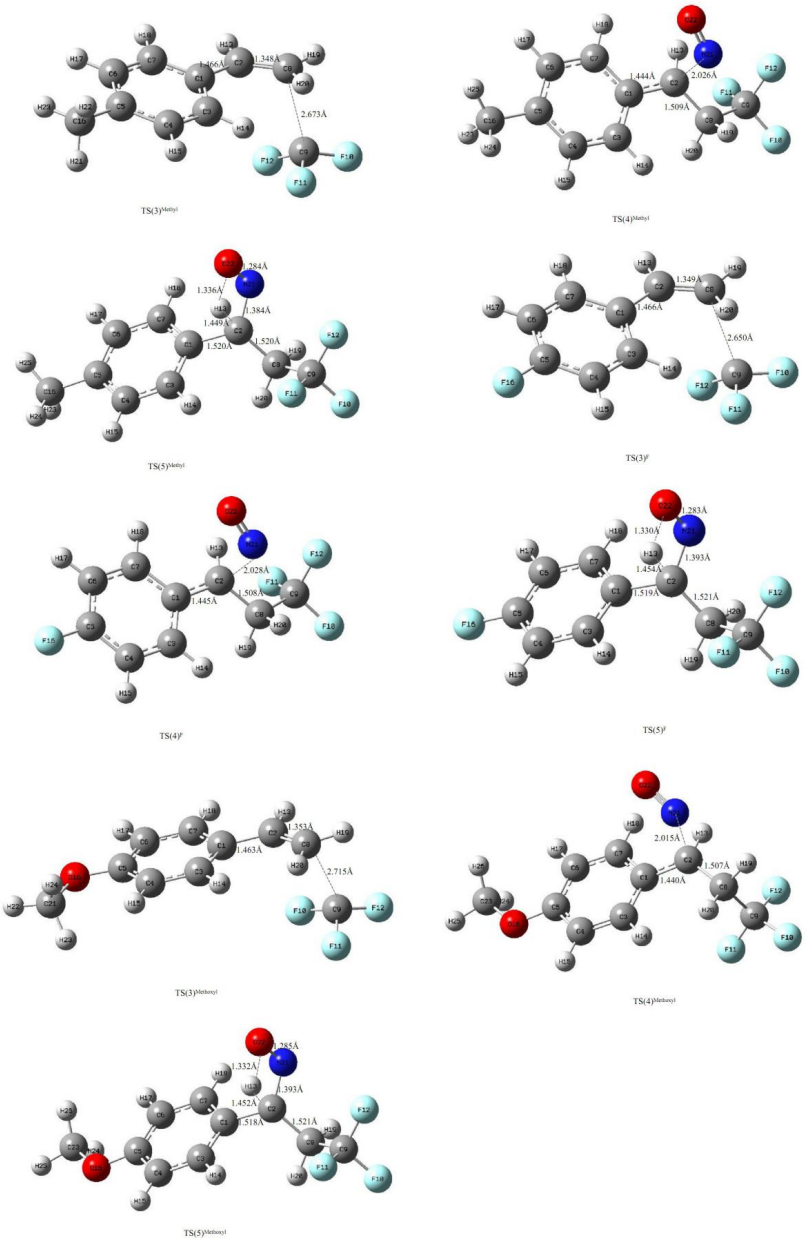

Figure 6. The optimized structure and some main parameters of the intermediates(IM), transition states(TS) and products(P) in steps of 4 5 and 6 of the difunctionalization reaction of para substituted styrene in vacuum.(Substituents marked as superscript. Oxygen:red; Nitrogen:blue; Carbon:gray; Fluorine:cyan; Hygrogen: white).

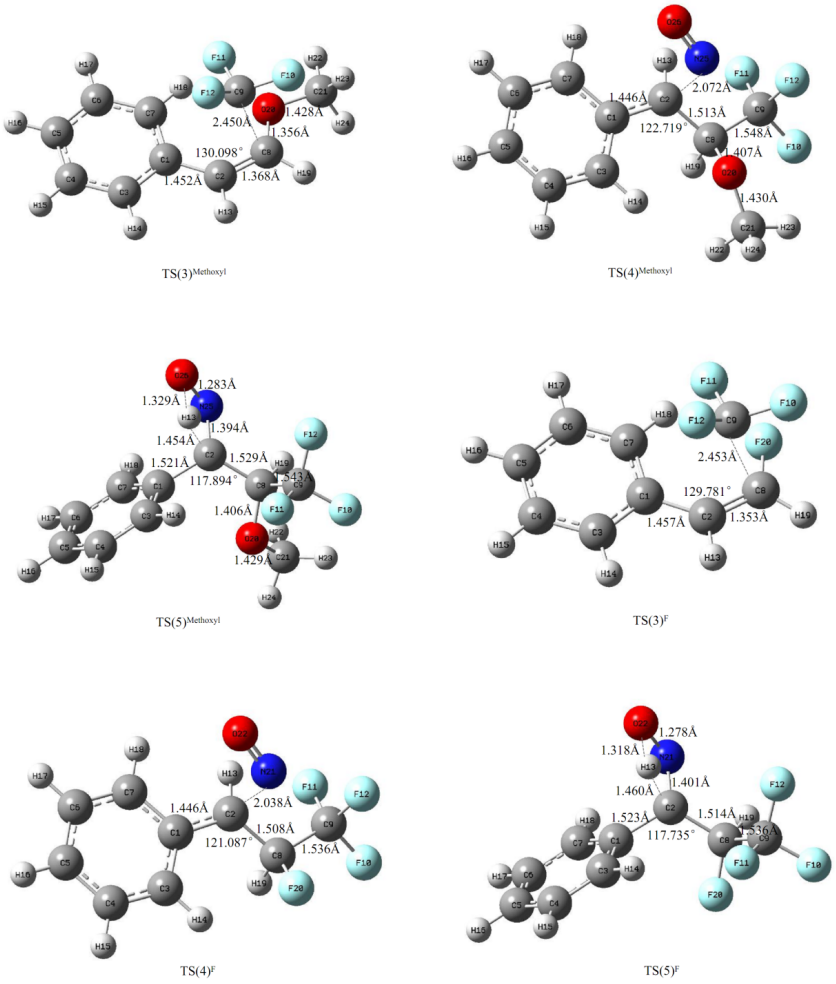

Figure 7. The optimized structure and some main parameters of the intermediates(IM), transition states(TS) and products(P) in steps of 4 5 and 6 of the difunctionalization reaction ofβ-C substituted styrene in vacuum (Substituents marked as superscript. Oxygen:red; Nitrogen:blue; Carbon:gray; Fluorine:cyan; Hygrogen: white).

3.4 The effect of the different solvents on the difunctionalization reaction

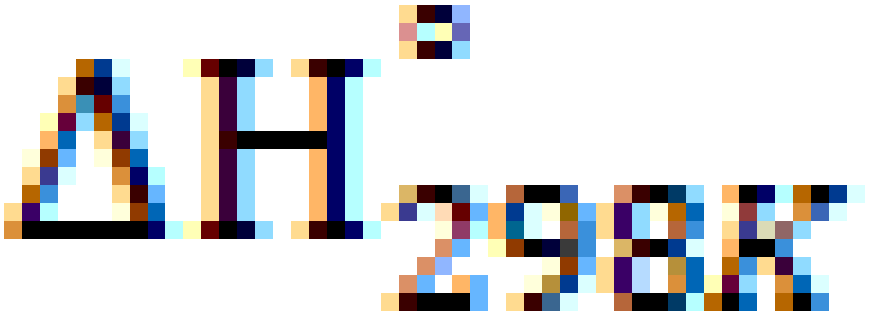

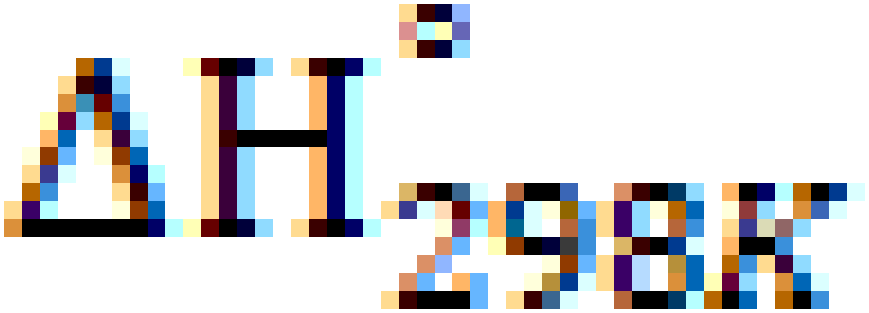

Generally, the solvent has significant effect on the reaction. In order to examine the solvent effect on the difunctionalization reaction of substituted styrenes, the difunctionalization reaction processes in DMSO, ethanol and water solvents were examined at B3LYP/6-31+G(d, p) level with CPCM solvent model. For styrene without any substituents, the energy barriers of the homolysis of TBN in DMSO, ethanol and water solvents were 47.88kcal/mol 47.86kcal/mol and 47.88kcal/mol respectively (given in table 1), which was 0.46kcal/mol 0.44kcal/mol and 0.46kcal/mol higher than that in vacuum respectively. The reaction rate constants of the homolysis of TBN are $3.558\times10^{-24}s^{-1}3.680\times10^{-24}s^{-1}$ and $3.558\times10^{-24}s^{-1}$ respectively. In this section, the subsequent value order given corresponds one-to-one to the solvent order with the former in DMSO, the middle in ethanol and the latter in water. The optimized structures of reactants, transitions and intermediates of the first process were similar to the data presented in vacuum. It was found that the presence of solvent is not conducive to the homolysis reaction of TBN because the energy barriers only changed a little. Step 2 is still a barrierless process in the solvent(potential energy surface scans are not provided), and their reaction enthalpy changes are 27.35kcal/mol 27.27kcal/mol and 27.36kcal/mol respectively. Subsequently, the generated $CF_3SO_2\cdot$ was homolyzed to give the $\cdot CF_3$ and SO_2. The energy barriers of the breakage of C-S bond are 4.97kcal/mol 4.99kcal/mol and 4.96kcal/mol respectively. The energy barriers in the third step are 0.71kcal/mol 0.69kcal/mol and 0.72kcal/mol lower than that in vacuum respectively. And in the solvents, the reaction rate constants are $9.859\times10^{7}s^{-1}9.531\times10^{7}s^{-1}$ and $1.002\times10^{8}s^{-1}$ respectively. The optimized structures of intermediates, transitions and products with some main structural parameters in the second reaction process of the difunctionalization reaction of styrene are very similar, so only the structure diagrams in DMSO are listed in Figure 8. By comparing the energy barriers of step 4 in vacuum with that in the solvents, we find that the energy barriers in the DMSO and ethanol are 0.75kcal/mol and 0.74kcal/mol lower than that in vacuum respectively. But in aqueous solvents, the energy barrier increases by 8.8kcal/mol. In the presence of solvents, the reaction energy barriers in step 5 are reduced by 1.93kcal/mol 1.88kcal/mol and 1.95kcal/mol respectively. The energy barriers of the rate-limiting step (step 6) in solvents

are all 58.36kcal/mol and the rate constants are all $3.771\times10^{-31}s^{-1}$. From the Gibbs free energy change() in Table 1, we can see that the Gibbs free energy changes of all the steps in solvent are decreased except for the first and the second steps.

The solvent effect on the reactions with substituted styrenes as reactants was also examined. Figures 9 and 10 show the optimized structures of the transition states with some main structural parameters of substituted styrenes in the second reaction process of the difunctionalization reaction in the solvent of DMSO. In other solvents, the optimized structures of the transition states are very similar to that in DMSO and are not listed here. The energy barriers and reaction rate constants of all steps in solvents are listed in Tables 2 and 3. And it can be seen that the solvents slightly increase the energy barrier at steps 4 and 6 and decrease that at step 5. This trend did not change with the position and type of the substituents in styrene.

In general, the solvent effect has little effect on the overall reaction. However, in solution, the molecules of the reactants can be dissolved and sufficiently contact to allow the reaction to proceed smoothly. DMSO has good solubility for most of the organic reactants and is helpful for the reactants to be sufficiently mixed to take the reaction. On the other hand, the energy barrier of final step of the reaction in this study is as high as 57.80kcal/mol and the energy barrier of step 1 is 47.42kcal/mol in vacuum, indicating that this reaction should be carried out at a higher temperature, and the high boiling point of DMSO can provide a higher temperature environment to facilitate the reaction. Therefore, the actual reaction is chosen to be carried out in DMSO solvent[45].

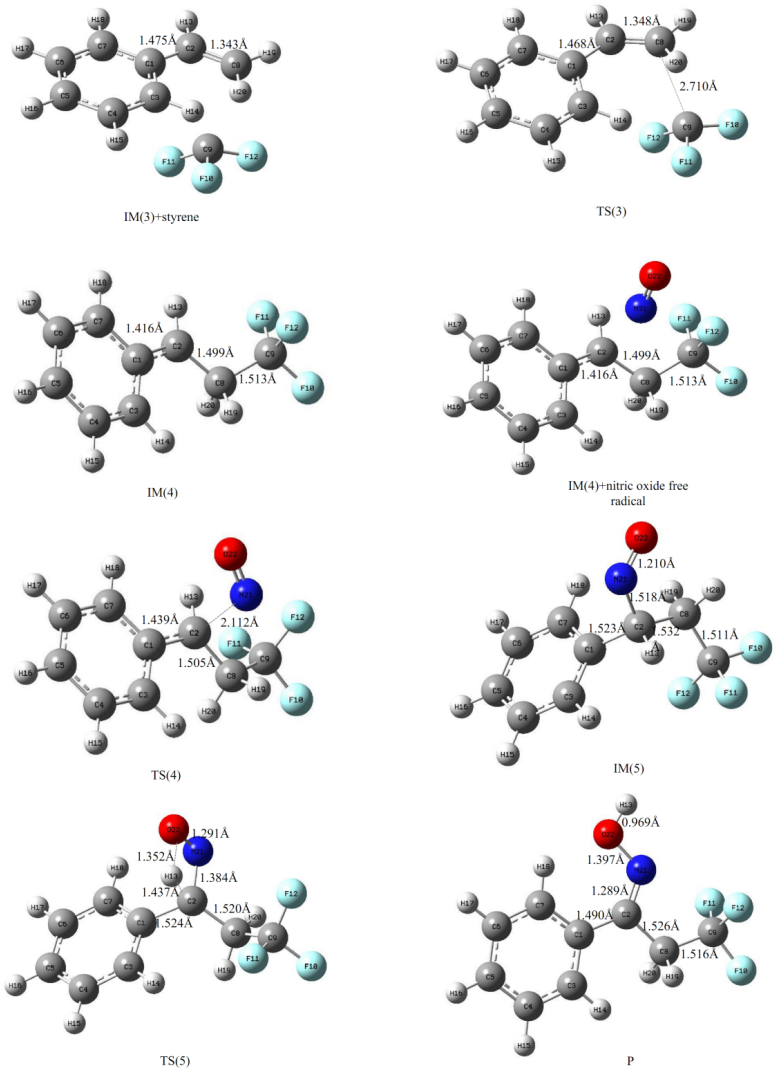

Figure 8. The optimized structure and some main parameters of the intermediates(IM), transition states(TS) and products(P) in steps of 4 5 and 6 of the difunctionalization reaction of styrene in DMSO(Oxygen:red; Nitrogen:blue; Carbon:gray; Fluorine:cyan; Hygrogen: white).

.

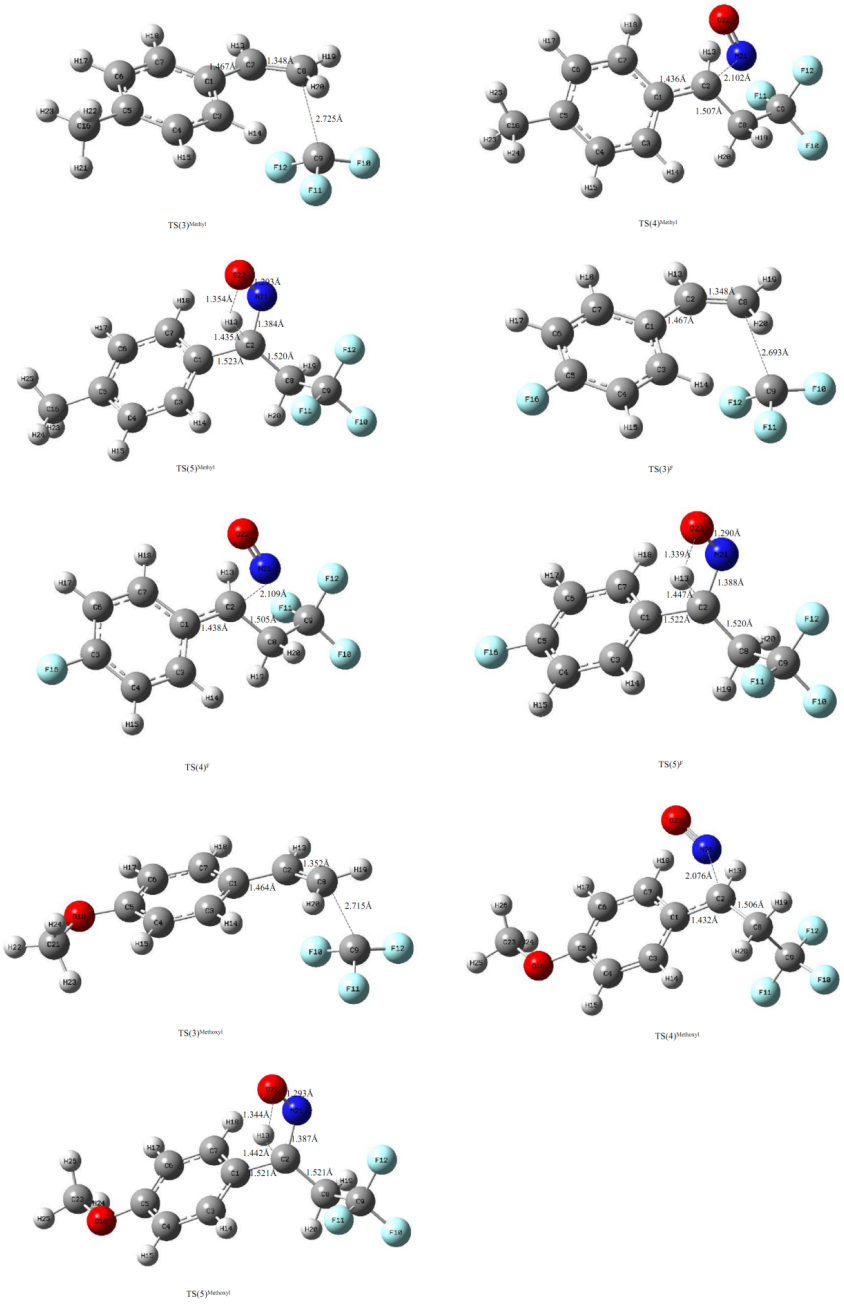

Figure 9. The optimized structure and some main parameters of the transition states(TS) in steps of 4 5 and 6 of the difunctionalization reaction for para substituted sterene in DMSO(Oxygen:red; Nitrogen:blue; Carbon:gray; Fluorine:cyan; Hygrogen: white).

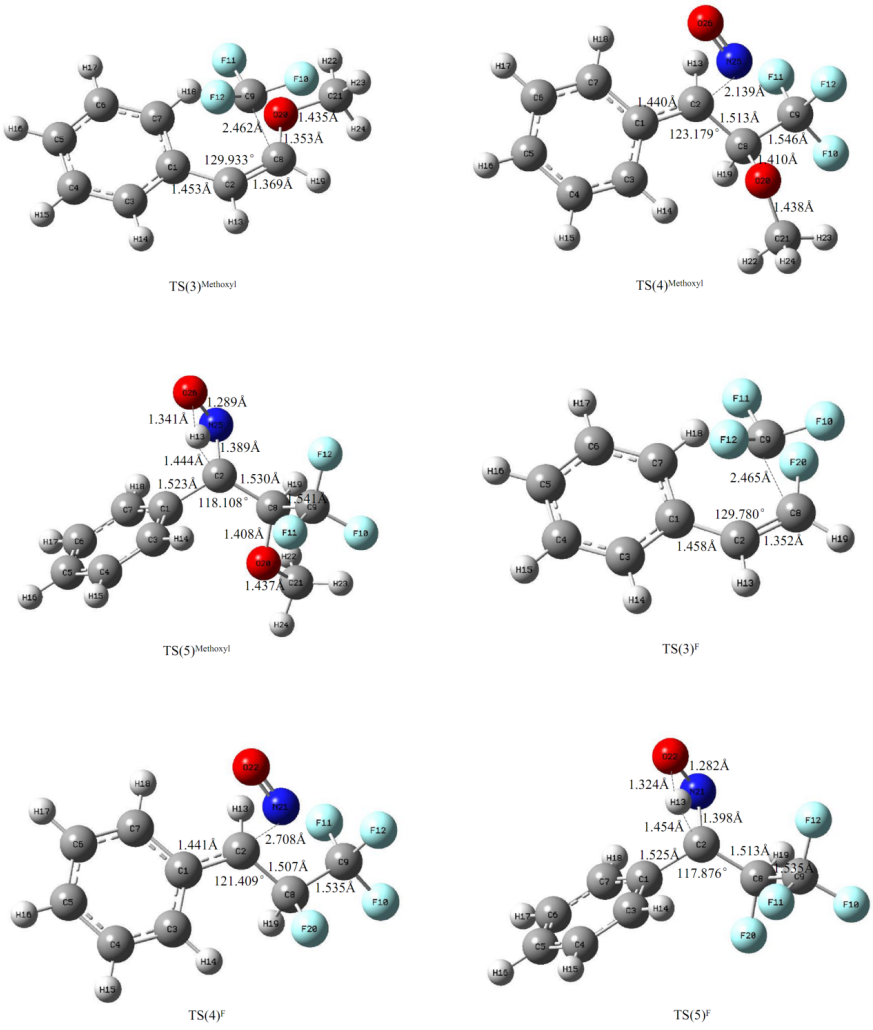

Figure 10. The optimized structure and some main parameters of the transition states (TS) in steps of 4 5 and 6 of the difunctionalization reaction for β-C substituted sterene in DMSO(Oxygen:red; Nitrogen:blue; Carbon:gray; Fluorine:cyan; Hygrogen: white).

3.5 Water mediated proton transfer in theoximation reaction

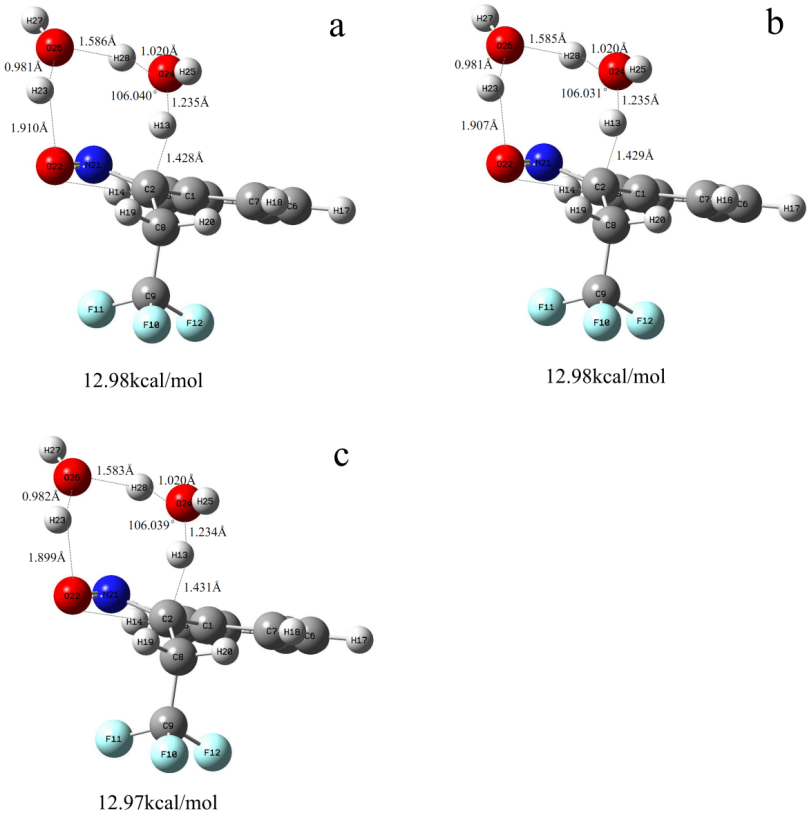

In the final step (step 6), the final oxime product was formed from the tautomerism of nitro compounds(such as IM(5)). It is a hydrogen transfer reaction. According to the homomolecular hydrogen transfer mechanism calculated previously (Step 6, the hydrogn transfer from α-C to O(22) directly to form the final product of oxime). It is the rate-limiting step with the highest energy barrier. With the mechanism calculations above, we found that neither substituents nor solvents had a significant effect on this rate-limiting step. However, there are many reports about the severe dercease of the energy barrier by water facilitated proton transfer. For examples, K Chuchev and X Cheng et al.[59, 60] reported that water molecules facilitate proton transfer in decarboxylation reaction. Many commonly used organic solvents also contain small amounts of water, which can also be used to facilitate the proton transfer of the reaction. Thus we calculated the water faciliated proton transfer in the tautomerism of nitro compound. When there is no water in vacuum, the proton is transferred through a C(2)-H(13)-O(22)-N(21) four-membered ring (As shown in Figure 5). The energy barrier for this transition state is 57.80kcal/mol in vacuum and it seriously slows down the overall reaction rate. When two water molecules are involved in the proton transfer in the water as shown in Figure 11(a), the transition state includes a seven-membered ring of (C(2)-H(13)-O(24)-H(28)-O(26)-H(23)-O(22)). H (13) transfer from C(2) to O(24) of the water molecule accompanied with H(28) of the water molecule approaching to the O(26) and meanwhile H(23) of the water molecule approaching to the O(22) of nitric oxide. With the aid of the two water molecules, proton transfer from C(2) to the O(22) of nitric oxide easily. (C(2) gives a proton to water but O(22) gets a proton from water). Lu Gao et al.[49] found that when a water molecule facilitate H transfer from carboxyl group to the a-C of benzene ring, energy barrier was lowered by 14.2kcal/mol. In this study, the energy barrier of step 6 with the two water molecules mediated proton transfer in the solvent of water is 12.98kcal/mol(shown in Figure 11(a)), which is 44.82kcal/mol lower than that in vacuum. In aqueous solvent, the energy barrier of proton transfer mediated with water in the final step is 45.38kcal/mol lower than that without water. It can be seen that the energy barrier was

significantly reduced by 77.8% when water was involved in the final step. However, in actual experimental process, organic solvents usually used for their better soulibility to organic reactants. The organic solvents used in the actual experimental process basically contain a small amount of water and some organic reagents are mutually soluble with water. So we then calculated the energy barrier changes of water mediated proton transfer in the final step in organic solvents of DMSO and ethanol. In the organic solvent of DMSO, the energy barrier decreases from 58.36kcal/mol to 12.98kcal/mol when water molecules participate in proton transfer. In ethanol solvent the energy barrier is reduced from 58.36kcal/mol to 12.97kcal/mol when water is involved in the proton transfer of step 6. These results show that the energy barrier of the final step was significantly reduced with the water existed in organic solvents, indicating that adding a small amount of water to the DMSO with better solubility to the reactants is conducive to the difunctionalization reaction.

Figure 11. The structural parameters and energy barriers of the transition states(TS) in step 6 with two water molecules mediated the proton transfer in the solvents of water(a), DMSO(b) and ethanol(c)(Oxygen:red; Nitrogen:blue; Carbon:gray; Fluorine:cyan; Hygrogen: white).

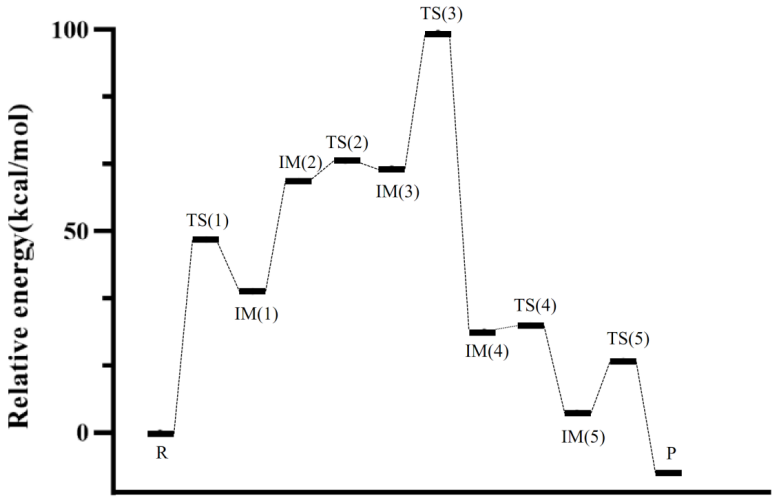

Figure 12. The potential energy surface of step 6 for two water molecules mediated the proton transfer in the solvent of water.

Conclusion

In the paper, the free radical reaction mechanism of the difunctionalization reaction on aryl-substituted ethylene was investigated by using Gaussian09 package at B3LYP/6-31+(d,p) level in vacuum and the solvent effect of DMSO, ethanol and water were examined with the CPCM solvent model. It was found that the step 2 of the formation of the $CF_3SO_2\cdot$(IM2) from reaction of CF_3SO_2Na with t-BuO$\cdot$ is a barrierless step, which can be carried out easily. The tautomerism reaction of 3,3,3-trifluoro-1-phenylpropan-1-nitric oxide(IM(5)) to the final product α-trifluoromethylethyl ketoxime(P) is the rate-limiting step (step 6). The substituents on para position of aryl ring and β-C do not influence the reaction rate significantly, which indicates that the reaction has a good adaptability to substrates containing different substituents, which has also been confirmed in experimental studies[45]. Based on our calculation, though the solvent effect does not influence the energy barrier of the tautomerism of step 6 significantly, the existence of water will change the reaction mechanism of step 6 and significantly reduces its energy barrier. The energy barrier of step 6 with the two water molecules mediated proton transfer in the solvent of water is 12.98kcal/mol, which is

44.82kcal/mol lower than that in vacuum and declined by 77.5%. When water participated in proton transfer in DMSO and ethanol, the energy barrier was also significantly reduced and declined by 77.7% and 77.8% respectively, indicating that the presence of a small amount of water in the organic solvents was conducive to the reaction. This study is of great significance for the application of bifunctionalized reaction in the synthesis of organic fluoride compounds with different substituents.

Acknowledgement

This study was financial supported by National Natural Science Foundation of Tianjin, grant No.19JCZDJC34800 and COVID-19 Prevention and Control Project of Tianjin University of Science and Technology (grant No.2020STCV0016).

Conflict of interest

We declare that we have no financial and personal relationships with other people or organizations that can inappropriately influence our work, there is no professional or other personal interest of any nature or kind in any product, service or company that could be construed as influencing the position presented in, or the review of, the manuscript entitled.

Reference

[1] Gad, S.C., Anderson, B., Kamrin, M., Hakkinen, P., Peyster, A.D. Encyclopedia of Toxicology; Second edition. 2005.

[2] Berger, R., Resnati, G., Metrangolo, P., Weber, E., Hulliger, J. Organic fluorine compounds: a great opportunity for enhanced materials properties. Cheminform. 2011, 40, 3496-508.

[3] Hagmann, William, K. The Many Roles for Fluorine in Medicinal Chemistry. Journal of Medicinal Chemistry. 2008, 51, 4359-69.

[4] Wang, J., Sánchez-Roselló, M., A Ce ?A, J.L., Pozo, C.D., Sorochinsky, A.E., Fustero, S., et al. Fluorine in pharmaceutical industry: fluorine-containing drugs introduced to the market in the last decade (2001-2011). Chemical Reviews. 2014, 114, 2432-506.

[5] Mei, H., Han, J., Klika, K.D., Izawa, K., Soloshonok, V.A. Applications of fluorine-containing amino acids for drug design. European Journal of Medicinal Chemistry. 2019, 186, 111826.

[6] Mansour, F. Fluorine in Life Sciences: Pharmaceuticals, Medicinal Diagnostics, and Agrochemicals || Synthesis and applications of backbone-fluorinated amino acids. 2019, 325-47.

[7] Shah, P., Westwell, A.D. The role of fluorine in medicinal chemistry. Journal of Enzyme Inhibition & Medicinal Chemistry. 2007, 22, 527-40.

[8] Montserrat, Rueda-Becerril, Olivier, Mahé, Myriam, Drouin, et al. Direct C–F Bond Formation Using Photoredox Catalysis. Journal of the American Chemical Society. 2014, 136, 2637-41.

[9] Wang, Z.G., Hammond, G.B. Fluorinated building blocks. The discovery of a stable difluoroallenyl indium and the synthesis of gem-difluoroallenyl and -propargyl synthons in aqueous media. Journal of Organic Chemistry. 2010, 32, no-no.

[10] Okamura, K. Recent Advances in Organic Fluorine Chemistry. J.synth.org.chem.jpn. 2010, 16, 446-53.

[11] Hu, J., Umemoto, T. Fluorination || Fluorination of Alkenes and Alkynes for Preparing Alkyl Fluorides. 2017, 10.1007/978-981-10-1855-8, 1-35.

[12] β-Keto-ester chemistry and ketolides. synthesis and antibacterial activity of 2-halogeno, 2-methyl and 2,3 enol-ether ketolides. Bioorganic & Medicinal Chemistry Letters. 2000.

[13] Peng, W., Zhu, S. Efficient Synthesis of 5-Fluoroalkylated 1H-1,2,3-Triazoles and Application of the Bromodifluoromethylated Triazole to Prepare New gem-Difluorinated Triazole Compounds. ChemInform.

2003, 34, 4395-404.

[14] Quantification of the Activation Capabilities of Lewis/Brnsted Acid for Electrophilic Trifluoromethylthiolating Reagents. Chinese Journal of Chemistry. 2020.

[15] Xue, X.S., Zhang, J., Yang, J.D., Zheng, H., Herbert, M., Cheng, J.P. Exploration of the Synthetic Potential of Electrophilic Trifluoromethylthiolating and Difluoromethylthiolating Reagents. Angewandte Chemie International Edition. 2018, 57.

[16] Qing, S. Syntheses and Applications of Trifluoromethyl- and Pentafluorosulfanyl-Containing Organic Molecules. 2017.

[17] Ogawa, Y., Tokunaga, E., Kobayashi, O., Hirai, K., Shibata, N. Current contributions of organofluorine compounds to the agrochemical industry. iScience. 2020, 101467.

[18] Inoue, M., Sumii, Y., Shibata, N. Contribution of Organofluorine Compounds to Pharmaceuticals. ACS Omega. 2020, XXXX.

[19] Design, Synthesis, and Antibacterial and Antifungal Activities of Novel Trifluoromethyl and Trifluoromethoxy Substituted Chalcone Derivatives. 2020.

[20] Wu, L.H., Zhao, K., Shen, Z.L., Loh, T.P. Copper-catalyzed trifluoromethylation of styrene derivatives with CF3SO2Na. Organic Chemistry Frontiers. 2017, 10.1039.C7QO00416H.

[21] Wang, X., Truesdale, L., Yu, J.Q. Pd(II)-catalyzed ortho-trifluoromethylation of arenes using TFA as a promoter. Journal of the American Chemical Society. 2010, 132, 3648–9.

[22] Hafner, D., Br?Se, P. Ortho-Trifluoromethylation of Functionalized Aromatic Triazenes. Angewandte Chemie International Edition. 2012, 51, 3713-5.

[23] Shen, C., Xu, J., Ying, B., Zhang, P. Heterogeneous Chitosan@Copper(II)-Catalyzed Remote Trifluoromethylation of Aminoquinolines with the Langlois Reagent by Radical Cross-Coupling. Chemcatchem. 2016, 8, 3559-.

[24] Li, Y., Wu, L., Neumann, H., Beller, M. Copper-catalyzed trifluoromethylation of aryl- and vinylboronic acids with generation of CF3-radicals. Chemical Communications. 2013, 49, 2628-30.

[25] ChemInform Abstract: Copper-Catalyzed Trifluoromethylation of Aryl- and Vinylboronic Acids with Generation of CF3-Radicals. Cheminform. 2013.

[26] Xu, J., Luo, D.F., Xiao, B., Liu, Z.J., Gong, T.J., Fu, Y., et al. Copper-catalyzed trifluoromethylation of aryl boronic acids using a CF3+ reagent. Chemical Communications. 2011, 47, p.4300-2.

[27] Hafner, A., Br?Se, S. Efficient Trifluoromethylation of Activated and Nonctivated Alkenyl Halides by Using (Trifluoromethyl)trimethylsilane. Advanced Synthesis & Catalysis. 2011, 353, 3044-8.

[28] Zhengbiao, He, Tao, Luo, Mingyou, Hu, et al. Copper-Catalyzed Di- and Trifluoromethylation of α,β-Unsaturated Carboxylic Acids: A Protocol for Vinylic Fluoroalkylations. Angewandte Chemie International Edition. 2001.

[29] Huang, P., Li, Y., Fu, X., Zhang, R., Jin, K., Wang, W., et al. Silver(I)-catalyzed denitrative trifluoromethylation of β-nitrostyrenes with CF 3 SO 2 Na. Tetrahedron Letters. 2016, 4705-8.

[30] Feng, Z., Min, Q., Zhao, H., Gu, J., Zhang, X. A General Synthesis of Fluoroalkylated Alkenes by Palladium-Catalyzed Heck-Type Reaction of Fluoroalkyl Bromides. Angewandte Chemie International Edition. 2014.

[31] Straathof, N., Cramer, S.E., Hessel, V., No?L, T. Practical Photocatalytic Trifluoromethylation and Hydrotrifluoromethylation of Styrenes in Batch and Flow. Angewandte Chemie. 2016.

[32] Sera, Y., Adachi, K., Fujii, K., Shizuri, Y. A new antifouling hexapeptide from a Palauan sponge, Haliclona sp. Journal of Natural Products. 2003, 66, 719-21.

[33] Duan, X.J., Li, X.M., Wang, B.G. Highly Brominated Mono- and Bis-phenols from the Marine Red Alga Symphyocladia latiuscula with Radical-Scavenging Activity. Journal of Natural Products. 2007, 70, 1210-3.

[34] Bergstr?M, M.A., Andersson, S.I., Broo, K., Luthman, K., Karlberg, A.T. Oximes: metabolic activation and structure-allergenic activity relationships. Journal of Medicinal Chemistry. 2008, 51, 2541-50.

[35] Qu, Hong-En, Liu, Liangxian, Wang, Heng-Shan, et al. Synthesis and pharmacological evaluation of novel bisindole derivatives bearing oximes moiety: Identification of novel proapoptotic agents. European Journal of Medicinal Chemistry Chimie Therapeutique. 2015.

[36] Yang, S.H., Chang, S. Highly efficient and catalytic conversion of aldoximes to nitriles. Organic Letters. 2001, 3, 4209-11.

[37] Dong, X., Kita, Y., Oestreich, M. Kinetic Resolution of alpha-Hydroxy-Substituted Oxime Ethers by Enantioselective Cu-H-Catalyzed Si-O Coupling. Angewandte Chemie International Edition. 2018.

[38] Wan, P.H., Iosub, A.V., Stahl, S.S. Pd-catalyzed Semmler-Wolff reactions for the conversion of substituted cyclohexenone oximes to primary anilines. Journal of the American Chemical Society. 2014, 45, 13664-7.

[39] Yamaguchi, K., Fujiwara, H., Ogasawara, Y., Kotani, M., Mizuno, N. A tungsten-tin mixed hydroxide as an efficient heterogeneous catalyst for dehydration of aldoximes to nitriles. Angewandte Chemie. 2010, 38, no-no.

[40] Sukhorukov, A.Y., Ioffe, S.L. Chemistry of Six-Membered Cyclic Oxime Ethers. Application in the Synthesis of Bioactive Compounds. Cheminform. 2011, 42, 5004-41.

[41] Knifton, J., F. Homogeneous catalyzed reduction of nitro compounds. I. Synthesis of oximes. Journal of Organic Chemistry. 1973, 38, 3296-301.

[42] Zeynizadeh, B., Karimkoshteh, M. Magnetic Fe3O4 nanoparticles as recovery catalyst for preparation of oximes under solvent-free condition. Journal of Nanostructure in Chemistry. 2013, 3, 57.

[43] Ji, Y., Liu, Y., Song, R., Peng, Z., Li, J. Copper-Mediated 1,2-Difunctionalization of Styrenes with Sodium Arylsulfinates and tert-Butyl Nitrite: Facile Access to α-Sulfonylethanone Oximes. Advanced Synthesis & Catalysis. 2016, 358.

[44] Chen, F., Zhou, N.N., Zhan, J.L., Han, B., Yu, W. tert-Butyl nitrite-mediated vicinal sulfoximation of alkenes with sulfinic acids: a highly efficient approach toward α-sulfonyl ketoximes. Organic Chemistry Frontiers. 2016, 10.1039.C6QO00535G.

[45] Lu, K., Wei, X., Li, Q., Li, Y., Zhao, X. Synthesis of α-Trifluoromethyl Ethanone Oximes via the Three-component Reaction of Aryl-substituted Ethylenes, tert-Butyl Nitrite, and the Langlois Reagent. Organic Chemistry Frontiers. 2019.

[46] Becke, A.D.P. Density-functional exchange-energy approximation with correct asymptotic behavior. Physical Review A. 1988, 38, 3098-100.

[47] Gaussview Users Manual. 2000.

[48] Marenich, A.V., Cramer, C.J., Truhlar, D.G. Universal Solvation Model Based on Solute Electron Density and on a Continuum Model of the Solvent Defined by the Bulk Dielectric Constant and Atomic Surface Tensions. Journal of Physical Chemistry B. 2009, 113, 6378-96.

[49] Gao, L., Hu, Y., Zhang, H., Liu, Y., Song, Z., Dai, Y. DFT computational study on decarboxylation mechanism of salicylic acid and its derivatives in the anionic state. Journal of Molecular Structure. 2016, 1116, 56-61.

[50] Quantum mechanical transition state theory and a new semiclassical model for reaction rate constants. Journal of Chemical Physics. 1974, 61, 1823-34.

[51] KiSThelP: a program to predict thermodynamic properties and rate constants from quantum chemistry results. Journal of Computational Chemistry. 2013, 35, 82-93.

[52] TSTcalculator.

[53] Liu, Y.P., Lu, D.H., Gonzalez-Lafont, A., Truhlar, D.G., Garrett, B.C. Direct dynamics calculation of the kinetic isotope effect for an organic hydrogen-transfer reaction, including corner-cutting tunneling in 21 dimensions. Journal of the American Chemical Society. 1993, 115, 7806-17.

[54] Dennington, R., Keith, T., Millam, J. GaussView 5.0, Gaussian. Inc., Wallingford. 2008.

[55] Zhu, X., Gao, Y., Wang, X., Haribal, V., Li, F. A tailored multi-functional catalyst for ultra-efficient styrene production under a cyclic redox scheme. Nature Communications. 2021, 12, 1329.

[56] Liang, Y., Taya, A., Zhao, Z., Saito, N., Shibata, N. Deoxyfluorination of acyl fluorides to trifluoromethyl compounds by FLUOLEAD /Olah's reagent under solvent-free conditions. Beilstein journal of organic chemistry. 16, 3052-8.

[57] Grainger, R., Cornella, J., Blakemore, D.C., Larrosa, I., Campanera, J.M. The ortho-Substituent Effect on the Ag-Catalysed Decarboxylation of Benzoic Acids. Chemistry. 2015, 20.

[58] Yanying, Hu, Lu, Gao, Zhoutong, Dai, et al. DFT investigation on the decarboxylation mechanism of ortho hydroxy benzoic acids with acid catalysis. Journal of Molecular Modeling. 2016, 22, 56.

[59] Chuchev, K., Belbruno, J.J. Mechanisms of decarboxylation of ortho-substituted benzoic acids. Journal of Molecular Structure THEOCHEM. 2007, 807, 1-9.

[60] Cheng, X., Wang, J., Ke, T., Liu, Y., Liu, C. Decarboxylation of pyrrole-2-carboxylic acid: A DFT investigation. Chemical Physics Letters. 2010, 496, 36-41.